Int J Cardiovasc Imaging
DOI 10.1007/s10554-011-0004-2

ORIGINAL PAPER

Iterative reconstruction of dual-source coronary CT angiography: assessment of image quality and radiation dose

Eun-Ah Park · Whal Lee · Kwang Woo Kim · Kwang Gi Kim · Allmendinger Thomas · Jin Wook Chung · Jae Hyung Park

Received: 20 September 2011 / Accepted: 14 December 2011

Abstract To assess the image quality and radiation dose of low-dose dual-source CT (DSCT) coronary angiography reconstructed using iterative reconstruction in image space (IRIS), in comparison with routine-dose CT using filtered back projection (FBP). Eighty-one patients underwent low-dose coronary DSCT using IRIS with two protocols: (a)100 kVp and 200 mAs per rotation for body mass index (BMI) < 25 (group I), (b)100 kVp and 320 mAs for BMI ≥ 25 (II). For comparison, two sex-and BMI-matched groups using standard protocols with FBP were selected: (a)100 kVp and 320 mAs for BMI < 25 (III), (b)120 kVp and 320 mAs for BMI ≥ 25 (IV). Image noise, signal to noise ratio (SNR) and modulation transfer function (MTF) 50% were objectively calculated. Two blinded readers then subjectively graded the image quality. Radiation dose was also measured. Image noise tended to be lower in IRIS of low-dose protocols: 22.0 ± 4.5 for group I versus 24.8 ± 4.0 for III ($P < 0.001$); 20.9 ± 4.5 for II versus 21.6 ± 4.9 for IV ($P = 0.6$). SNR was better with IRIS: 25.8 ± 4.4 for I versus 22.7 ± 4.6 for III ($P < 0.001$); 24.6 ± 5.4 for II versus 18.7 ± 4.5 for IV ($P < 0.001$). No differences in MTF 50% or image quality scores were seen between each two groups ($P > 0.05$). Radiation reduction was 40% for I and 51% for II, compared to standard protocols. Compared with routine-dose CT using FBP, low-dose coronary angiography using IRIS provides significant radiation reduction without impairment to image quality.

Keywords Cardiac CT · Iterative reconstruction · Radiation dose · Dual-source CT · Coronary angiography

Abbreviations

CT	Computed tomography
FBP	Filtered back projection
ASIR	Adaptive statistical iterative reconstruction
IRIS	Iterative reconstruction in image space
BMI	Body mass index
DSCT	Dual-source CT
Bpm	Beats per minute

E.-A. Park · W. Lee (✉) · K. W. Kim · J. W. Chung · J. H. Park
Department of Radiology, Seoul National University Hospital, Seoul 110-744, Korea
e-mail: whal.lee@gmail.com

E.-A. Park · W. Lee · K. W. Kim · J. W. Chung · J. H. Park
SNU-Duke Cardiovascular MR Research Center, Seoul National University, Seoul 110-744, Korea

K. G. Kim
Biomedical Engineering Branch, Division of Convergence Technology, National Cancer Center, Goyang-si, Gyeonggi-do 410-769, Korea

A. Thomas
Siemens Medical Solution AG-computed Tomography, Forchheim, Germany

Published online: 21 December 2011

SNR	Signal-to-noise ratio
CNR	Contrast-to noise ratio
ROI	Region of interest
MTF	Modulation transfer function
$CTDI_{vol}$	Volume CT dose index
DLP	Dose length product

Introduction

Dose reduction techniques of computed tomography (CT), such as anatomy-adapted tube current modulation [1], low tube voltage [2–9], noise reduction filters [10] and optimization of z-axis scan length [3] for general application, as well as ECG pulsing [11], heart rate-adaptive pitch [12], sequential ECG triggering [9, 13] and high pitch acquisition [14] for cardiac application, have been successfully shown to reduce radiation exposure while generating acceptable image quality. However, further reductions in radiation dose are hindered by increased image noise and degraded image quality mainly as a result of the limitations of the standard filtered back projection (FBP) reconstruction algorithm currently used on all CT scanners. When using this conventional technique of reconstructing raw data into image data, a fixed connection between spatial resolution and image noise exists, with higher spatial resolution being directly correlated to increased image noise.

As iterative reconstruction approaches theoretically allow the decoupling of this correlation between spatial resolution and image noise, a wide variety of iterative reconstruction approaches have been developed in the last 20 years. However, although iterative reconstruction has been widely used in positron emission tomography, it has only recently been introduced to CT and has been handicapped due to the slow convergence process of reconstruction and, consequently, demand for more robust computing power. Recently, the first modified and computationally faster iterative reconstruction technique based on only one statistical corrective model, adaptive statistical iterative reconstruction (ASIR), was newly introduced, and the published data suggest that radiation dose could indeed be significantly reduced using ASIR [15–21].

Now, another method for iterative reconstruction (iterative reconstruction in image space, IRIS; Siemens) has been developed. The new IRIS algorithm generates a "master" image only once from raw data not like the classic iterative reconstruction in which the reconstructions from the raw data are performed numerous times. The following iterative corrections known from theoretical iterative reconstruction are consecutively performed in image space based on the "master" image. They remove the image noise without degrading image sharpness. Therefore, the time-consuming repeated projection and corresponding back projection from the raw data can be avoided. In this study, we hypothesized that IRIS would allow for additional reduction in tube current and tube voltage, resulting in further radiation dose reduction for coronary CT angiography with acceptable image noise without degrading image sharpness.

Materials and methods

This retrospective study was approved by our institutional review board and the requirement for informed consent was waived due to retrospective manners of this study.

Study population

From May to June 2010, two different low-dose protocols of coronary CT angiography were applied according to body mass index (BMI): (a) 100 kVp and 200 mAs per rotation in patients with a BMI of less than 25 (group I; 56 subjects) and (b) 100 kVp and 320 mAs per rotation or more in patients with a BMI of 25 or greater (group II; 25 subjects). For comparison, two sex- and BMI-matched groups using standard protocols were selected in reverse chronological order from April to March 2010 by one investigator (E. A. P): (a) 100 kVp and 320 mAs per rotation in patients with a BMI of less than 25 (group III; 56 subjects) and (b) 120 kVp and 320 mAs per rotation or more in patients with a BMI of 25 or greater (group IV; 25 subjects). BMI matching was performed by using a tight BMI difference limit; mean difference 0.084 ± 0.512. The investigator was allowed access to clinical information, but was blinded to CT image data. Finally, 162 subjects, 78 men (mean age, 60.7 years ± 9.9; range, 30–83 years) and 84 women (mean age, 61.8 years ± 9.9; range, 37–83 years) with an overall mean age of 61.3 years ± 9.9 ranging from 30 to 83 years, were

enrolled in this study: 24 men and 32 women for groups I and III, respectively; and 15 men and 10 women for groups II and IV, respectively. All patients were referred for clinically indicated CT coronary angiography and additional iterative reconstruction images were obtained in all patients.

CT protocol

All CT examinations were performed using a dual-source CT (DSCT) scanner (Somatom Definition; Siemens Medical Solutions, Forchheim, Germany). Patients with a pre-scan heart rate of 65 beats per minute (bpm) or higher were given 50–100 mg of oral metoprolol (Betaloc; AstraZeneca, Sweden) 45–60 min prior to the CT examination, unless the subject had a contraindication to beta-blockers. Additional beta-blockers were not administered to any subjects who underwent CT scanning 45–60 min after administration of beta-blockers, even if the heart rate was not decreased to below 65 bpm.

Precontrast scanning for calcium scoring was performed using prospective ECG-triggering with 80% of R–R interval protocol (3-mm section thickness and collimation, 120 kVp, tube current–time 100 mAs, collimation, 32 × 0.6 mm; section acquisition, 64 × 0.6 mm with the z-flying focal spot technique; gantry rotation time, 330 ms; pitch, 0.2–0.5, depending on the heart rate).

A total of 0.4 mg of Sublingual nitroglycerin (Nitroquick; Ethex, St. Louis, Mo) was administered in all subjects except two who had a contraindication to nitroglycerin for coronary vasodilation after completion of calcium scoring scanning. 60 mL of a nonionic contrast medium (Ultravist 370; Shering, Berlin, Germany) was injected into an antecubital vein at 5 mL/s, followed by an additional 20 mL of a nonionic contrast medium and 50 mL of an 8:2 mixture of normal saline and contrast medium, at a flow rate of 4 mL/s with the use of a dual power injector (Stellant; Medrad, Indianola, Pa). The bolus triggering method was used to determine the beginning point of CT acquisition by monitoring the signal density of the contrast medium in the mid-ascending aorta. CT scans were started 8 s after a threshold trigger of 150 HU above baseline was reached.

All scans were performed from the level of the tracheal bifurcation to the diaphragm in a caudocranial direction with a detector collimation of 32 × 0.6 mm, section collimation of 64 × 0.6 mm with a z-flying focal spot, gantry rotation time of 330 ms, and adaptive pitch of 0.2–0.5 depending on the heart rate. Pitch was adjusted to the lowest expected heart rate while scanning. For the low dose protocols, two different parameters were used according to BMI: in patients with a BMI of less than 25, a tube voltage of 100 and maximum tube current–time of 200 mAs per rotation was used; in patients with a BMI of 25 or greater, a tube voltage of 100 and maximum tube current–time of 320–360 mAs per rotation was used. For the standard protocols as well, two different parameters were used according to BMI: in patients with a BMI of less than 25, a tube voltage of 100 and maximum tube current–time of 320 mAs per rotation was used; in patients with a BMI of 25 or greater, a tube voltage of 120 and maximum tube current–time of 320–380 mAs per rotation was used.

A retrospective ECG-gated technique with a mono-segment reconstruction algorithm was used for image reconstruction. The ECG-pulsing window for radiation dose reduction was applied in all patients: 65 ~ 75% of R–R interval in patients with ≤65 beats/min and 25 ~ 80% for in patients with >65. Outside the ECG-pulsing window, the tube current was reduced to 4% of the full current (Mindose; Siemens Healthcare). Standard reconstruction algorithms were applied by using an absolute reverse or percentage technique to obtain data sets during end systole and/or mid- to end diastole according to heart rate. Retrospective ECG-gated image reconstruction was performed with a half-scan and single RR-interval reconstruction algorithm, providing for a temporal resolution of 83 ms. The first image reconstruction was performed at 70% of the RR-cycle, followed by an automatically generated reconstruction using dedicated reconstruction software, which automatically generates the most quiescent phase during the RR-cycle by calculating a motion strength function between several reconstructions at low resolution over the cardiac cycle and identifying periods of low difference between neighboring phases (BestDiast/BestSyst, Siemens Medical Solutions). If motion artifacts were present, additional data sets were manually reconstructed. Image reconstruction windows were manually repositioned to achieve high image quality in patients with arrhythmia, as previously described by Oncel et al. [22].

Parameters used for image reconstruction for the DSCT coronary angiography included a slice thickness of 0.8 mm, increment of 0.4 mm, and a medium-soft convolution kernel (B26f for FBP and I26f for IRIS).

CT analysis

Evaluation of image noise and contrast

To obtain objective indices of image quality, we determined image noise, signal-to-noise ratio (SNR) [23], and contrast-to noise ratio (CNR) [23] in 0.8 mm thickness images of both FBP and IRIS algorithms for the four different scanning protocols. Image noise was derived from the standard deviation of the density values (in HU) with a 300 mm^2 sized region of interest (ROI) located in the ascending aorta. SNR was assessed in the sinus of Valsalva with an ROI of 50 mm^2 in area, by calculating the mean density of the sinus of Valsalva divided by image noise. CNR was defined as the difference between the mean density of the contrast-filled left ventricular chamber and the mean density of the left ventricular wall, which was then divided by image noise [23]. In terms of measuring the densities of the left ventricular wall, we measured the densities twice on the septal and lateral wall and averaged them. All measurements and calculations were performed by placing ROIs in the same location on both FBP and IRIS images by one investigator (K. W. K).

Evaluation of spatial resolution based on modulation transfer function

To determine the spatial resolution of images reconstructed with FBP and IRIS, we measured the modulation transfer function (MTF) 50%, i.e. the spatial frequency corresponding to 50% of MTF. MTF mathematically quantifies the frequency responses of various filters, providing quantitative assessment of spatial resolution [20]. MTF was calculated as the angular mean of the two-dimensional Fourier transform of the point-spread function measured from CT images [24]. The investigator (K. W. K) converted paired transverse images of FBP and IRIS techniques at the same location of the right coronary artery mid portion from dicom files to TIFF files. MTF 50% was measured twice by placing the ROI across the right coronary artery wall using a commercially available matlab 15.0 (The Mathworks Inc., Natick, MA), and then was averaged. The greater value of MTF 50% indicated better spatial resolution.

Subjective image quality analysis

Two independent, blinded and experienced readers (E. A. P. and W. L. with 7 and 9 years of coronary CT angiography experience, respectively) reviewed the 324 data sets (162 FBP and 162 IRIS images) in randomized order. Each reader assigned a Likert scale for each data set on the basis of preferred image quality, with a focus on image noise, coronary wall definition, and low contrast resolution. The readers were instructed to ignore issues such as respiratory motion and poor gating which could not be attributed to the reconstruction algorithm. The mean value of the Likert scores from the two readers was used for analysis. The Likert scale was defined as 1: poor, impaired image quality limited by excessive noise or poor vessel wall definition; 2: adequate, reduced image quality with poor vessel wall definition or excessive image noise, limitations in low contrast resolution evident; 3: good, moderate image noise, limitations of low contrast resolution and vessel margin definition are minimal; 4: very good, good attenuation of vessel lumen and delineation of vessel walls, relative image noise is minimal, coronary wall definition and low contrast resolution well maintained; and 5: excellent, excellent attenuation of the vessel lumen and clear delineation of the vessel walls, limited perceived image noise [19].

Radiation dose evaluation

Scan length was documented for every examination. Volume CT dose index ($CTDI_{vol}$) and dose length product (DLP), which were provided by the scanner system, were recorded. The estimated effective dose was derived from the DLP and a conversion coefficient for the chest as the investigated anatomic region. Different conversion factors (k) according to sex and voltage were applied based on ICRP publication 103: 0.0104 mSv mGy^{-1} cm^{-1} for adult male with use of 100 kV, 0.0105 for adult male with use of 120 kV, 0.0183 for female with use of 100 kV and 0.0185 female with use of 120 kV [25, 26].

Statistical analysis

Comparisons of paired results between FBP and IRIS images in each protocol were analyzed using the paired *t* test. Differences in clinical parameters and results between FBP images of the standard protocols and IRIS images of low-dose protocols according to BMI category were evaluated using the student *t* test.

All statistical analyses were performed with statistical packages (SPSS for Windows, version 17.0, SPSS, Chicago, Ill; GraphPad Prism, version 3.02, GraphPad Software, San Diego, Calif; MedCalc for Windows, version 8.1.0.0, MedCalc Software, Mariakerke, Belgium). Differences were considered significant when the *P* value was less than 0.05.

Results

Study group characteristics

There were no significant differences in patient age, heart rate, heart rate variability, and BMI between the groups (Table 1).

Comparison between FBP and IRIS images in same patients

In all patients, image noise significantly decreased from a mean of 26.3 ± 5.6 in FBP images to 19.9 ± 4.5 in IRIS images ($P < 0.001$), resulting in an average reduction of 24.3% (Fig. 1). On the other hand, mean densities of the sinus of Valsalva and left ventricular wall were similar in both images in all patients: 519.3 ± 103.3 HU in FBP and 519.5 ± 104.4 HU in IRIS for mean density of the sinus of Valsalva ($P = 0.793$); 128.4 ± 21.2 HU in FBP and 128.3 ± 21.1 HU in IRIS for left ventricular wall ($P = 0.341$). Both SNR and CNR were also significantly better in IRIS images than in FBP images in all patients: 20.3 ± 4.6 in FBP and 26.8 ± 5.7 in IRIS for SNR ($P < 0.001$); 14.2 ± 3.9 in FBP and 18.6 ± 4.8 in IRIS for CNR ($P < 0.001$). Similar trends were found in the comparison of paired results between FBP and IRIS images in each group (Fig. 2a, b, c, d).

Mean values of MTF 50% were 0.0283 ± 0.0030 for FBP images and 0.0290 ± 0.0029 for IRIS images in all patients. Although a significant difference was found ($P < 0.001$), mean differences in MTF 50% values of both images were very small, 0.0007 ± 0.0015. As shown in Fig. 2e, similar tendencies were noted in each group: MTF 50% of IRIS images was slightly better than that of FBP images.

Mean scores of subjective image quality was significantly better in IRIS images than in FBP images in all patients: 4.12 ± 0.62 in FBP and 4.49 ± 0.60 in IRIS images ($P < 0.001$). In each group, subjective image quality was also significantly better in IRIS images than in FBP images (all, $P < 0.05$) (Fig. 2f).

Table 2 provides the mean values of image quality parameters of each group in detail.

Comparison between FBP images of the standard protocol and IRIS images of the low-dose protocol

In the category of a BMI of less than 25, image noise was significantly lower in the IRIS images of the low-dose protocol than in the FBP images of the standard protocol ($P < 0.001$) (Fig. 2a). On the other hand, mean densities of sinus of Valsalva and left ventricular wall were similar in both images ($P > 0.005$) (Fig. 2b). Therefore, significant improvement of SNR

Table 1 Comparison of general features according to the four different groups

	Total	BMI less than 25			BMI 25 or greater		
		Low-dose protocol Group I	Standard protocol Group III	*P* value	Low-dose protocol Group II	Standard protocol Group IV	*P* value
No. patients	162	56	56		25	25	
Age	61.3 ± 9.9	60.6 ± 11.5	61.0 ± 9.3	0.863	64.3 ± 9.1	60.4 ± 8.1	0.111
HR	61.0 ± 9.7	60.7 ± 10.5	61.8 ± 9.1	0.572	61.1 ± 10.0	60.1 ± 9.5	0.718
HR variability	10.1 ± 14.6	8.1 ± 8.3	11.1 ± 16.7	0.235	12.4 ± 15.5	9.9 ± 19.4	0.620
BMI	24.7 ± 3.2	22.8 ± 1.4	22.8 ± 1.4	0.947	28.6 ± 2.1	28.9 ± 2.2	0.609

HR heart rate, *BMI* body mass index

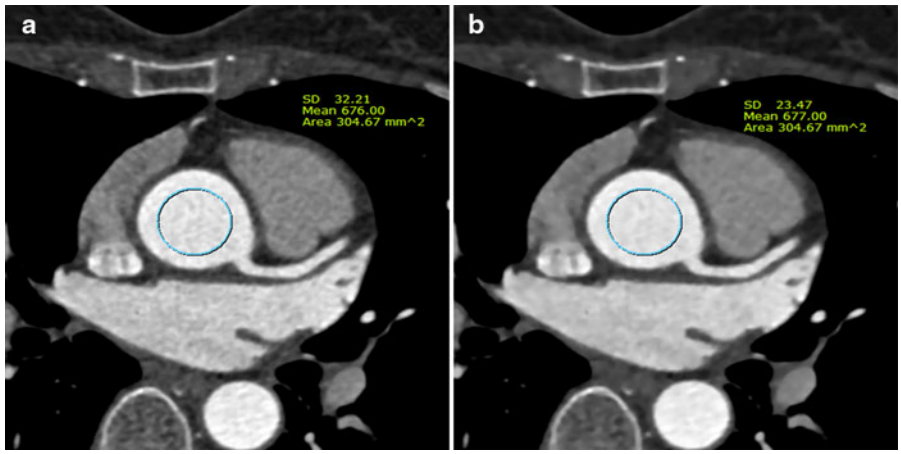

Fig. 1 CT images of a 56-year-old female: filtered back projection (FBP) (**a**) and iterative reconstruction in image space (IRIS) (**b**) CT densities of the ascending aorta were similar in both images but image noise was decreased in the IRIS image

and CNR was found in IRIS images of the low-dose protocol, compared to those in FBP images of the standard protocol (all, $P < 0.001$) (Fig. 2c, d). There were no significant differences in MTF 50% values between both data sets ($P = 0.913$) (Fig. 2e). On subjective analysis of image quality, there were no significant differences between IRIS and FBP images ($P = 0.546$) (Fig. 2f).

In the category of a BMI of 25 or greater, image noise was similar between IRIS images of the low-dose protocol and FBP images of the standard protocol ($P = 0.609$) (Fig. 1a). Of note, mean densities of sinus of Valsalva and left ventricular wall were significantly higher in IRIS images of the low-dose protocol than in FBP images of the standard protocol (Fig. 2b). Therefore, significant improvement of SNR and CNR was found in the IRIS images of the low-dose protocol, compared to those in the FBP images of the standard protocol (all, $P < 0.01$) (Fig. 2c, d). There were no significant differences in MTF 50% values between both data sets ($P = 0.533$) (Fig. 2e). On subjective analysis of image quality, there were no significant differences between IRIS and FBP images ($P = 1.0$) (Fig. 3).

Reduction of radiation dose

Mean scan ranges were slightly longer in the standard protocols than in the low-dose protocols but the difference did not reach a statistical significance ($P > 0.05$) (Table 3). Table 3 summarizes the comparison of radiation dose estimation between standard and low-dose protocols according to BMI category. In the category of a BMI of less than 25, $CTDI_{vol}$, DLP, and mean effective dose showed an average reduction of 39.2, 39.3, and 39.7%, respectively, in the low-dose protocol compared to the standard protocol. In the category of a BMI of 25 or greater, $CTDI_{vol}$, DLP, and mean effective dose showed an average reduction of 49.8, 50.0, and 51.3%, respectively, in the low-dose protocol compared to the standard protocol.

Discussion

The principal findings of the present study can be summarized as follows: (1) IRIS images significantly improved objective and subjective image quality by reducing image noise compared with FBP images, (2) spatial resolution based on calculation of MTF did not decrease when using the IRIS reconstruction technique. On the contrary, MTF 50% (spatial resolution) improved with statistical significance in the IRIS images compared with the FBP images although the difference was small, (3) in patients with a BMI of less than 25, IRIS images provided 40% radiation reduction without any impairment to image quality by reducing the tube current from 320 mAs per rotation to 200 mAs per rotation, and (4) in patients with a BMI of 25 or greater, IRIS images provided 51% radiation reduction without any impairment to image quality by reducing the tube voltage from 120 to 100 kVp.

The IRIS approach is based on an initial "master" FBP reconstruction with a very sharp convolution

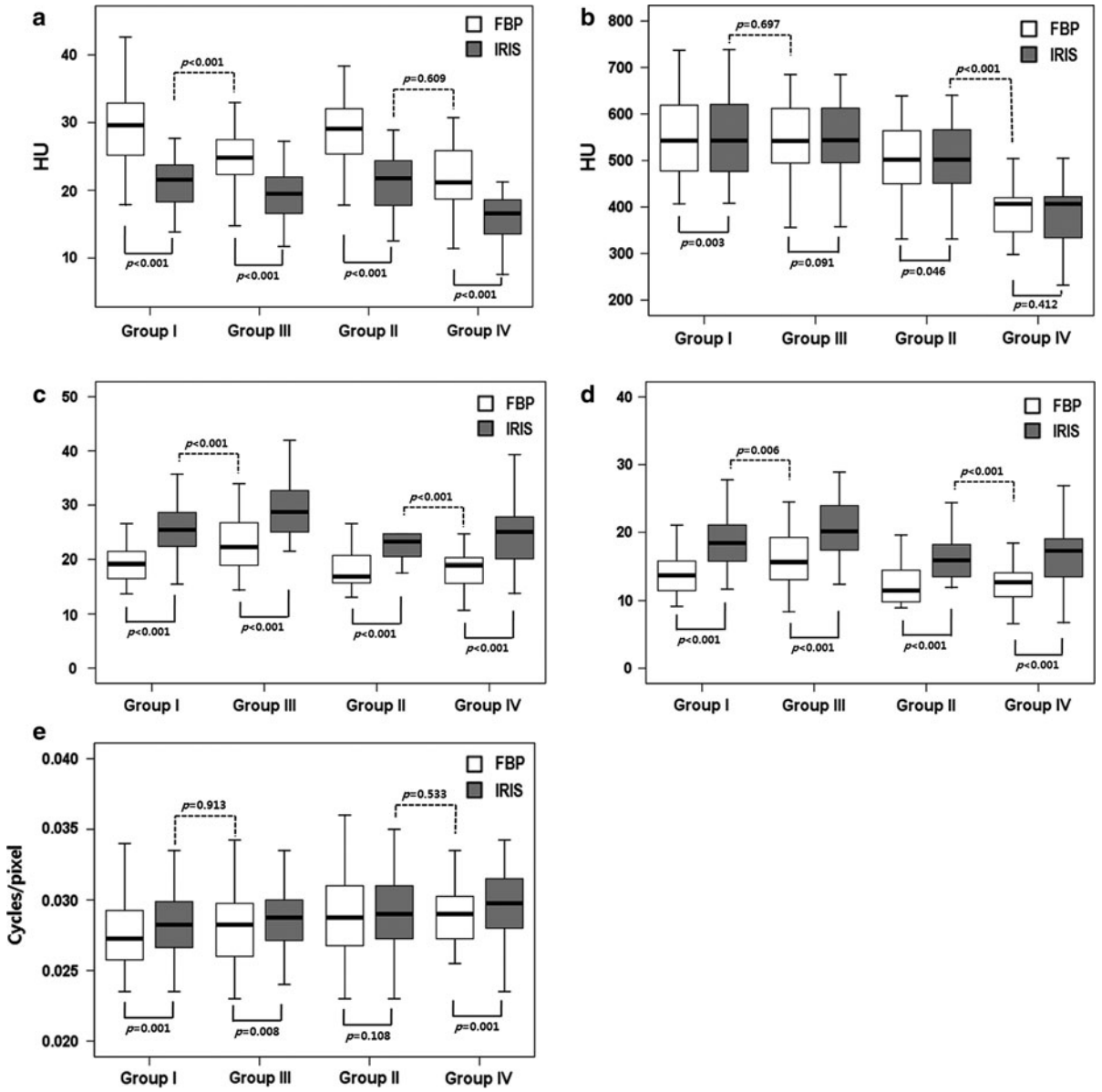

Fig. 2 Boxplots of objective measurements of both filtered back projection (FBP) and iterative reconstruction in image space (IRIS) images according to the four different protocols. **a** Image noise, **b** Densities of the sinus of Valsalva, **c** Signal to noise ratio, **d** Contrast to noise ratio, and **e** Modulation transfer function 50%. A *thick horizontal line* in the center of *each box* indicates the median of mean values. *Thin horizontal lines* at the *top* and *bottom* of each box indicate the minimum and maximum values. The *boxplot* itself represents interquartile range. Group I, low-dose protocol using 100 kVp and 200 mAs per rotation in patients with a body mass index (BMI) of less than 25, Group II, standard dose protocol using 100 kVp and 320 mAs or more per rotation in patients with a BMI of less than 25, Group III, low-dose protocol using 100 kVp and 320 mAs per rotation in patients with a BMI of 25 or greater, and Group IV, standard dose protocol using 120 kVp and 320 mAs or more per rotation in patients with a BMI of 25 or greater

kernel still containing all the frequencies and, thereby, all the information of the initial raw data. Subsequent iterative processing loops are applied to the image volume in which the image noise is reduced while sharpness is preserved depending on the physical properties of the scanner system and the reconstruction

Table 2 Results of image noise, contrast, modulation transfer function, and image quality

A: BMI less than 25	Low-dose protocol		Standard protocol	
	Group I		Group III	
	FBP	IRIS	FBP	IRIS
Image noise (HU)	29.2 ± 5.2	22.0 ± 4.5	24.8 ± 4.0	19.2 ± 3.5
Sinus Valsalva density (HU)	556.7 ± 92.7	557.7 ± 92.9	551.2 ± 84.3	551.9 ± 83.9
Left ventricular wall (HU)	135.1 ± 20.1	135.1 ± 20.1	133.4 ± 18.6	133.2 ± 18.4
SNR	19.5 ± 3.7	25.8 ± 4.4	22.7 ± 4.6	29.4 ± 5.8
CNR	13.8 ± 3.4	18.3 ± 4.2	16.1 ± 4.0	20.8 ± 4.8
MTF 50% (cycles/pixel)	0.0278 ± 0.0028	0.0285 ± 0.0025	0.0284 ± 0.0034	0.0290 ± 0.0031
Image quality	3.93 ± 0.60	4.32 ± 0.61	4.39 ± 0.62	4.79 ± 0.41
B: BMI 25 or greater	Low-dose protocol		Standard protocol	
	Group II		Group IV	
	FBP	IRIS	FBP	IRIS
Image noise (HU)	28.2 ± 5.8	20.9 ± 4.5	21.6 ± 4.9	14.6 ± 5.8
Sinus Valsalva density (HU)	496.8 ± 87.2	497.4 ± 87.1	386.7 ± 58.9	383.3 ± 62.2
Left ventricular wall (HU)	125.5 ± 19.7	125.5 ± 19.7	104.8 ± 11.8	104.8 ± 11.8
SNR	18.1 ± 4.0	24.6 ± 5.4	18.7 ± 4.5	25.1 ± 6.5
CNR	12.4 ± 3.0	16.8 ± 3.9	12.3 ± 3.7	16.6 ± 5.0
MTF 50% (cycles/pixel)	0.0288 ± 0.0032	0.0293 ± 0.0032	0.0288 ± 0.0025	0.0300 ± 0.0030
Image quality	4.00 ± 0.41	4.28 ± 0.54	4.12 ± 0.62	4.49 ± 0.60

HU Hounsfield unit, *SNR* signal to noise ratio, *CNR* contrast to noise ratio, *MTF* modulation transfer function, *FBP* filtered back projection, *IRIS* iterative reconstruction in image space

parameters. On the other hand the noise model is generated from the raw data. The general image properties, e.g., edge information and contrast-to-noise ratio are analyzed based on a noise model and applied to the so-called regularization step. The result from each regularization stepis compared to the initial data leading to an updated image, which is added to the previous dataset before the next iteration is performed. Therefore the iterative loops enable significant noise reduction while preserving edge information and low-contrast structures. The iterative reconstruction is performed in the image domain, the time consuming classical iterative reconstruction approaches in which the reconstruction form the raw data sets is necessary (Fig. 4). Most importantly, our data showed that spatial resolution of IRIS images was not impaired during the process of significant noise reduction. Recently, several studies using IRIS have been reported [27–35]. They consistently reported that IRIS enables significant reduction of image noise without loss of diagnostic information in comparison to FBP images and suggested potential for reducing radiation exposure [27–29, 32, 34, 35]. Further, two studies using IRIS in the application of chest and abdomen reported radiation reduction at 35 and 50% dose, respectively [30, 31], which results are similar to ours.

Our study also showed that using the IRIS technique was able to reduce both tube current or tube voltage without impairment to image quality, providing a tool to obtain additional dose reduction to established dose reduction techniques. Tube current reduction in CT is typically expected to result in increased image noise due to the decreased number of photons; however, despite the tube current reduction, images reconstructed with IRIS had no significant increase in image noise when compared with FBP images. Furthermore, with tube voltage reduction, the IRIS technique becomes a more powerful technique as radiation exposure can decrease exponentially not linearly by reducing tube voltage. Several studies on the usefulness of low kVp in coronary CT angiography have already been published [2, 3, 5, 6, 8, 9, 23]. As the

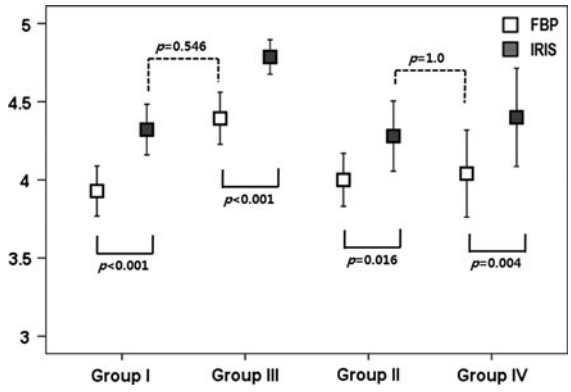

Fig. 3 Graph of subjective image quality of both filtered back projection (FBP) and iterative reconstruction in image space (IRIS) images according to the four different protocols. *Box* indicates mean values of subjective image quality between the two images. *Thin horizontal lines* at the *top* and *bottom* of *each box* indicate standard deviation. Group I, low-dose protocol using 100 kVp and 200 mAs per rotation in patients with a body mass index (BMI) of less than 25, Group II, standard dose protocol using 100 kVp and 320 mAs or more per rotation in patients with a BMI of less than 25, Group III, low-dose protocol using 100 kVp and 320 mAs per rotation in patients with a BMI of 25 or greater, and Group IV, standard dose protocol using 120 kVp and 320 mAs or more per rotation in patients with a BMI of 25 or greater

lower photon energy at lower X-ray tube voltages causes higher attenuation levels of iodinated contrast media, using a low kVp may permit a substantial increase in vessel signal intensity, and thus might compensate for the higher image noise [4, 7, 8]. Therefore, for low tube voltage protocols, investigators generally use 80 kVp for slim patients and 100 kVp for patients with normal weight [4, 6, 9]. Yet, radiologists still hesitate to use 100 kVp for patients with a high BMI over 25, as they remain suspicious as to whether high vessel density can overcome the higher image noise in overweight patients [2, 6]. In this situation, IRIS images of low tube voltage protocols can efficiently work to improve image quality by reducing image noise. The use of iterative reconstruction techniques is expected to increase in CT as computational processing continues to improve and algorithms become more robust and easy to apply [19]. As more powerful iterative reconstruction algorithms start to emerge, we may see greater noise reduction and thereby permit further reduction in current radiation dose [19]. Indeed, CT vendors are now providing their own iterative reconstruction algorithms. Recently, several studies using ASIR have

Table 3 Comparison of radiation dose estimations between groups

A: BMI less than 25			
	Low-dose protocol Group I	Standard protocol Group III	*P* value
Parameters	100 kVp 200 mAs	100 kVp 320 mAs	
$CTDI_{vol}$ (mGy)	15.0 ± 3.7	24.7 ± 8.8	<0.001
DLP (mGy cm)	242.1 ± 65.7	399.2 ± 156.6	<0.001
Effective dose (mSv)	3.6 ± 1.3	6.0 ± 3.0	<0.001
Scan range (mm)	128.9 ± 10.2	130.7 ± 12.6	0.385
B: BMI 25 or greater			
	Low-dose protocol Group II	Standard protocol Group IV	*P* value
Parameters	100 kVp 320–360 mAs	120 kVp 320–380 mAs	
$CTDI_{vol}$ (mGy)	24.6 ± 8.2	49.0 ± 15.7	<0.001
DLP (mGy cm)	384.6 ± 129.9	769.0 ± 251.2	<0.001
Effective dose (mSv)	5.2 ± 2.2	10.7 ± 5.1	<0.001
Scan range (mm)	125.4 ± 9.5	127.6 ± 9.4	0.419

BMI body mass index, *$CTDI_{vol}$* Volume CT dose index, *DLP* dose-length product

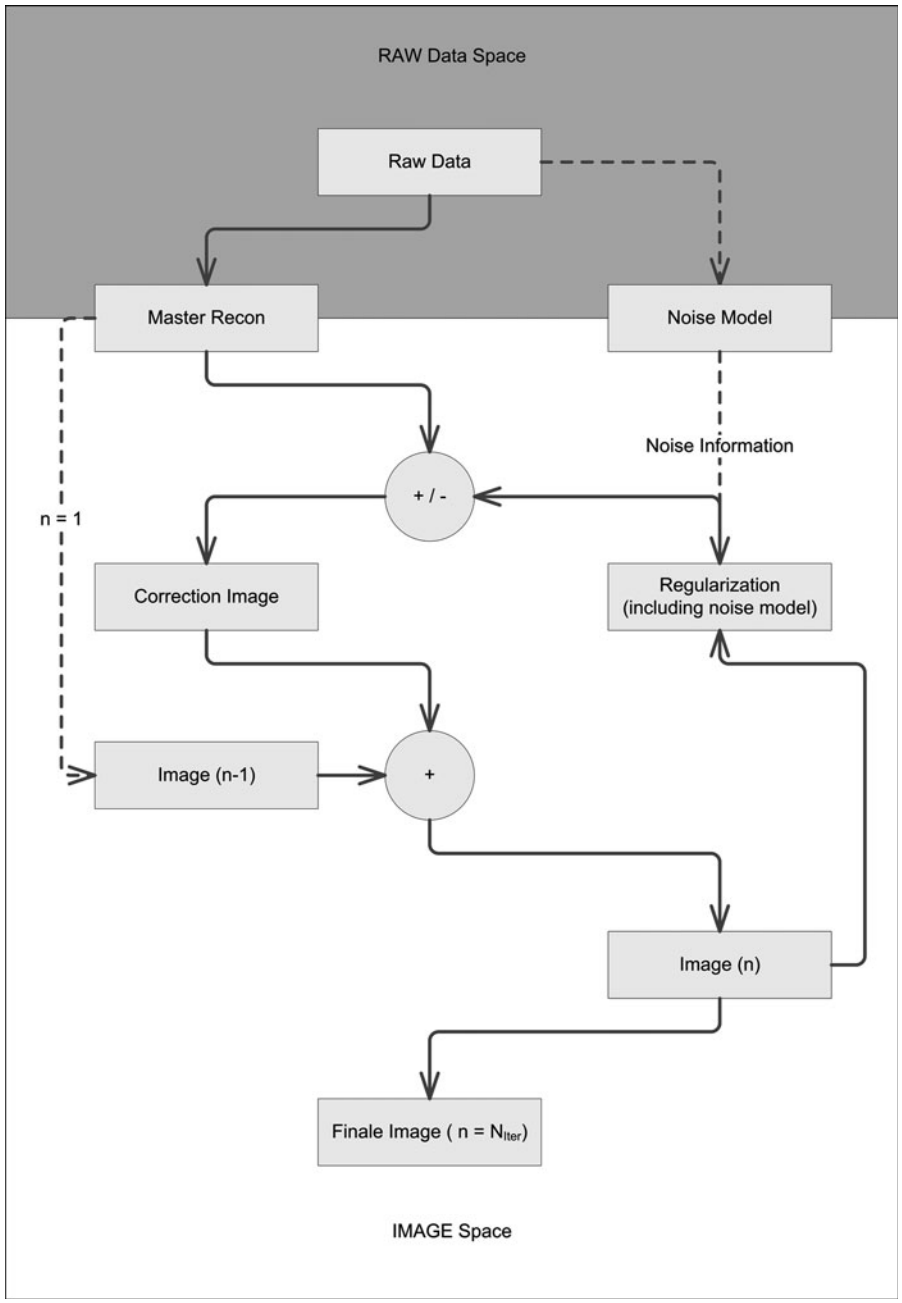

Fig. 4 Simple diagram of method for iterative reconstruction in image space

also been reported, including application of ASIR in the imaging of the lung, heart, abdomen and colon [15–21], and they have consistently found a significant improvement of image quality of iterative reconstruction compared to that of the FBP technique [15, 18, 20]. They also found that radiation dose can be significantly reduced using ASIR [16, 17, 19, 21]. Several technical issues still remain, however. One issue is that the noise texture of the images is notably different from standard FBP reconstruction, and thus may limit its use, as operators must become accustomed to working with these unfamiliar image impressions. Another issue is the determination of the optimal combination of iterative reconstruction

and FBP as aggressive noise reduction causes a noise-free appearance with unusually homogeneous attenuation [18].

There are several limitations to this study. First, although we used sex-and BMI-matched data in order to minimize confounding factors, for obvious ethical reasons, we could not compare signal and dose parameters in an intra-individual fashion. Therefore, the size of the breast in the female was not matched and thus differences in body habitus may have contributed to variations in signal and noise measurements. Second, individual hemodynamic differences may have influenced our study results, even though the bolus tracking method was used in all subjects in order to optimize contrast-agent injection. Third, diagnostic accuracy was not measured for the detection of coronary artery disease. Therefore, we were not able to verify that IRIS images of low-dose protocol would improve accuracy in the detection of coronary artery disease.

In conclusion, low-dose coronary CT angiography using the IRIS technique provides significant radiation reduction without any impairment to image quality compared with routine-dose CT using FBP. IRIS allows additional reduction in tube current or tube voltage while decreasing image noise, resulting in further radiation reduction for coronary CT with acceptable image quality without degradation in image sharpness.

Acknowledgments This study was supported by a grant of the Korean Health Technology R&D Project, Ministry of Health & Welfare, Republic of Korea (No. A100131).

References

1. Kalender WA, Wolf H, Suess C, Gies M, Greess H, Bautz WA (1999) Dose reduction in CT by on-line tube current control: principles and validation on phantoms and cadavers. Eur Radiol 9:323–328
2. Hausleiter J, Martinoff S, Hadamitzky M, Martuscelli E, Pschierer I, Feuchtner GM, Catalan-Sanz P, Czermak B, Meyer TS, Hein F, Bischoff B, Kuse M, Schomig A, Achenbach S (2010) Image quality and radiation exposure with a low tube voltage protocol for coronary CT angiography results of the PROTECTION II Trial. JACC Cardiovasc Imag 3:1113–1123
3. LaBounty TM, Earls JP, Leipsic J, Heilbron B, Mancini GB, Lin FY, Dunning AM, Min JK (2010) Effect of a standardized quality-improvement protocol on radiation dose in coronary computed tomographic angiography. Am J Cardiol 106:1663–1667
4. Sigal-Cinqualbre AB, Hennequin R, Abada HT, Chen X, Paul JF (2004) Low-kilovoltage multi-detector row chest CT in adults: feasibility and effect on image quality and iodine dose. Radiology 231:169–174
5. Abada HT, Larchez C, Daoud B, Sigal-Cinqualbre A, Paul JF (2006) MDCT of the coronary arteries: feasibility of low-dose CT with ECG-pulsed tube current modulation to reduce radiation dose. AJR Am J Roentgenol 186:S387–S390
6. Leschka S, Stolzmann P, Schmid FT, Scheffel H, Stinn B, Marincek B, Alkadhi H, Wildermuth S (2008) Low kilovoltage cardiac dual-source CT: attenuation, noise, and radiation dose. Eur Radiol 18:1809–1817
7. Heyer CM, Mohr PS, Lemburg SP, Peters SA, Nicolas V (2007) Image quality and radiation exposure at pulmonary CT angiography with 100- or 120-kVp protocol: prospective randomized study. Radiology 245:577–583
8. Park EA, Lee W, Kang JH, Yin YH, Chung JW, Park JH (2009) The image quality and radiation dose of 100-kVp versus 120-kVp ECG-gated 16-slice CT coronary angiography. Korean J Radiol 10:235–243
9. Stolzmann P, Leschka S, Scheffel H, Krauss T, Desbiolles L, Plass A, Genoni M, Flohr TG, Wildermuth S, Marincek B, Alkadhi H (2008) Dual-source CT in step-and-shoot mode: noninvasive coronary angiography with low radiation dose. Radiology 249:71–80
10. McCollough CH, Primak AN, Saba O, Bruder H, Stierstorfer K, Raupach R, Suess C, Schmidt B, Ohnesorge BM, Flohr TG (2007) Dose performance of a 64-channel dual-source CT scanner. Radiology 243:775–784
11. Weustink AC, Mollet NR, Pugliese F, Meijboom WB, Nieman K, Heijenbrok-Kal MH, Flohr TG, Neefjes LA, Cademartiri F, de Feyter PJ, Krestin GP (2008) Optimal electrocardiographic pulsing windows and heart rate: effect on image quality and radiation exposure at dual-source coronary CT angiography. Radiology 248:792–798
12. Weustink AC, Neefjes LA, Kyrzopoulos S, van Straten M, Neoh Eu R, Meijboom WB, van Mieghem CA, Capuano E, Dijkshoorn ML, Cademartiri F, Boersma E, de Feyter PJ, Krestin GP, Mollet NR (2009) Impact of heart rate frequency and variability on radiation exposure, image quality, and diagnostic performance in dual-source spiral CT coronary angiography. Radiology 253:672–680
13. Shuman WP, Branch KR, May JM, Mitsumori LM, Lockhart DW, Dubinsky TJ, Warren BH, Caldwell JH (2008) Prospective versus retrospective ECG gating for 64-detector CT of the coronary arteries: comparison of image quality and patient radiation dose. Radiology 248:431–437
14. Sommer WH, Albrecht E, Bamberg F, Schenzle JC, Johnson TR, Neumaier K, Reiser MF, Nikolaou K (2010) Feasibility and radiation dose of high-pitch acquisition protocols in patients undergoing dual-source cardiac CT. AJR Am J Roentgenol 195:1306–1312
15. Yanagawa M, Honda O, Yoshida S, Kikuyama A, Inoue A, Sumikawa H, Koyama M, Tomiyama N (2010) Adaptive statistical iterative reconstruction technique for pulmonary CT image quality of the cadaveric lung on standard- and reduced-dose CT. Acad Radiol 17:1259–1266
16. Flicek KT, Hara AK, Silva AC, Wu Q, Peter MB, Johnson CD (2010) Reducing the radiation dose for CT

colonography using adaptive statistical iterative reconstruction: a pilot study. AJR Am J Roentgenol 195:126–131
17. Hara AK, Paden RG, Silva AC, Kujak JL, Lawder HJ, Pavlicek W (2009) Iterative reconstruction technique for reducing body radiation dose at CT: feasibility study. AJR Am J Roentgenol 193:764–771
18. Leipsic J, Labounty TM, Heilbron B, Min JK, Mancini GB, Lin FY, Taylor C, Dunning A, Earls JP (2010) Adaptive statistical iterative reconstruction: assessment of image noise and image quality in coronary CT angiography. AJR Am J Roentgenol 195:649–654
19. Leipsic J, Labounty TM, Heilbron B, Min JK, Mancini GB, Lin FY, Taylor C, Dunning A, Earls JP (2010) Estimated radiation dose reduction using adaptive statistical iterative reconstruction in coronary CT angiography: the ERASIR study. AJR Am J Roentgenol 195:655–660
20. Prakash P, Kalra MK, Ackman JB, Digumarthy SR, Hsieh J, Do S, Shepard JA, Gilman MD (2010) Diffuse lung disease: CT of the chest with adaptive statistical iterative reconstruction technique. Radiology 256:261–269
21. Sagara Y, Hara AK, Pavlicek W, Silva AC, Paden RG, Wu Q (2010) Abdominal CT: comparison of low-dose CT with adaptive statistical iterative reconstruction and routine-dose CT with filtered back projection in 53 patients. AJR Am J Roentgenol 195:713–719
22. Oncel D, Oncel G, Tastan A (2007) Effectiveness of dual-source CT coronary angiography for the evaluation of coronary artery disease in patients with atrial fibrillation: initial experience. Radiology 245:703–711
23. Hausleiter J, Meyer T, Hadamitzky M, Huber E, Zankl M, Martinoff S, Kastrati A, Schomig A (2006) Radiation dose estimates from cardiac multislice computed tomography in daily practice: impact of different scanning protocols on effective dose estimates. Circulation 113:1305–1310
24. Efstathopoulos EP, Costaridou L, Kocsis O, Panayiotakis G (2001) A protocol-based evaluation of medical image digitizers. Br J Radiol 74:841–846
25. Deak PD, Smal Y, Kalender WA (2010) Multisection CT protocols: sex- and age-specific conversion factors used to determine effective dose from dose-length product. Radiology 257:158–166
26. Goo HW (2012) CT radiation dose optimization and estimation: an update for radiologists. Korean J Radiol 13:1–12 (in press)
27. Bittencourt MS, Schmidt B, Seltmann M, Muschiol G, Ropers D, Daniel WG, Achenbach S (2010) Iterative reconstruction in image space (IRIS) in cardiac computed tomography: initial experience. Int J Cardiovasc Imag (Epub ahead of print)
28. Fleischmann D, Boas FE (2011) Computed tomography–old ideas and new technology. Eur Radiol 21:510–517
29. Ghetti C, Ortenzia O, Serreli G (2011) CT iterative reconstruction in image space: a phantom study. Phys Med (Epub ahead of print)
30. May MS, Wust W, Brand M, Stahl C, Allmendinger T, Schmidt B, Uder M, Lell MM (2011) Dose reduction in abdominal computed tomography: intraindividual comparison of image quality of full-dose standard and half-dose iterative reconstructions with dual-source computed tomography. Invest Radiol 46:465–470
31. Pontana F, Duhamel A, Pagniez J, Flohr T, Faivre JB, Hachulla AL, Remy J, Remy-Jardin M (2011) Chest computed tomography using iterative reconstruction vs filtered back projection (Part 2): image quality of low-dose CT examinations in 80 patients. Eur Radiol 21:636–643
32. Pontana F, Pagniez J, Flohr T, Faivre JB, Duhamel A, Remy J, Remy-Jardin M (2011) Chest computed tomography using iterative reconstruction vs filtered back projection (Part 1): Evaluation of image noise reduction in 32 patients. Eur Radiol 21:627–635
33. Renker M, Nance JW Jr, Schoepf UJ, O'Brien TX, Zwerner PL, Meyer M, Kerl JM, Bauer RW, Fink C, Vogl TJ, Henzler T (2011) Evaluation of heavily calcified vessels with coronary CT angiography: comparison of iterative and filtered back projection image reconstruction. Radiology 260:390–399
34. Renker M, Ramachandra A, Schoepf UJ, Raupach R, Apfaltrer P, Rowe GW, Vogt S, Flohr TG, Kerl JM, Bauer RW, Fink C, Henzler T (2011) Iterative image reconstruction techniques: applications for cardiac CT. J Cardiovasc Comput Tomogr 5:225–230
35. Schindera ST, Diedrichsen L, Muller HC, Rusch O, Marin D, Schmidt B, Raupach R, Vock P, Szucs-Farkas Z (2011) Iterative reconstruction algorithm for abdominal multidetector CT at different tube voltages: assessment of diagnostic accuracy, image quality, and radiation dose in a phantom study. Radiology 260:454–462